Enhancement of Structural and Creep Properties of Sn-5 wt% Zn Solder Reinforced with Nano-metric Particles of Al_2O_3

A.M.Abd El-Khalek, A.S.Mahmoud and F.Fahim
A.M.Abd El-Khalek: Asaad Mohammed abd el-khalek,

Physics Department, Faculty of Education, Ain Shams University
Physics Department, Faculty of Education, Ain Shams University
Physics Department, Faculty of Education, Ain Shams University

Sn-Zn alloy has been taken as one of the most important lead free solder alloys due to toxicity and alpha radiation effects of lead impurities. Strain-time relations of Sn-5 wt.%Zn and Sn-5 wt.%Zn-0.5 wt.%Al_2O_3 alloys were obtained under different constant stresses (10-25 MPa) over a temperature range from 333 K to 393 K. The results of this study shows the transient creep parameters dependence on the testing temperature and the applied stress of both compounds. This work, study the effect of adding Al_2O_3 nano-particles to Sn-5 wt.%Zn on the thermal, structural and tensile creep properties. The addition of Al_2O_3 nano-particles slightly changed the thermal properties, but improved the tensile creep resistance.

1. Introduction:

In view of the environmental and health issues concerning the toxicity of Pb present in the most prominent Pb-Sn [1], much attention has been paid to the development of lead-free solder alloys which avoid the environmental problem of lead [2, 3]. The lead-free solder alloys are well known for their low melting point, excellent mechanical properties and low cost make them attractive as materials for electronic applications [4]. Pewters (pewter is an alloy of more than 90% Sn) because of their ease of fabrication into any required shape [5] is used mostly as solders for packing and interconnection in the electronic, electrical, and engineering industries. The solder alloy results are decreasing on being wetted with poor corrosion resistance of the alloy [6]. Studies on the composition of lead–free solder showed that the particle reinforcing is also an effective way to achieve the improvement of solder alloys. Generally, there are many kinds of adding reinforcements that are supposed, to enhance microstructure, thermal and mechanical properties of such lead free solder alloys. Some authors have tried to add a third element, such as; Bi, Ag, In, Ti and Ni, to modify the structural properties of Sn–Zn lead-free solders. For example, Kim et al [7] studied the

effect of Bi addition on thermal properties of Sn–Zn solder alloy. It was found that the melting point decreased with increasing Bi content. Saad et al. [8] reported that, with the addition of Ag to Sn–8.8 wt%Zn solder alloy, the minimum creep rate of Sn–8.8 wt%Zn and Ag containing alloy increases with the deformation temperature and applied stress. Other studies on some Sn-based alloys showed that their mechanical properties are controlled by their microstructure [9,10,11]. These studies investigated the effect of temperature gradient and growth rate on the mechanical, electrical and thermal properties during solidifications with different conditions.

Recently, lead-free solders doped with nano-sized, non-reacting, non-coarsening oxide dispersoids have been identified as potential materials to provide high microstructure stability and better mechanical properties as compared to conventional solders. Mavoori and Jin [12] studied Pb37Sn composite solder with 10 nm Al_2O_3 and 5 NM TiO_2 reinforcement particles and reported significant improvements in its mechanical properties. Mechanical measurements reported significant increases in microhardness, offset yield strength (0.2 %YS), and ultimate tensile strength (UTS). However, the ductility decreased with increasing amounts of TiO_2 nano-sized particles. Tsao et al. [12-13] reported significant improvement in the mechanical response after adding: (1) nano-sized TiO_2 particles on Sn3-5Ag-0.25Cu [13], and (2) nano-sized Al_2O_3 on Sn3_5Ag_5Cu lead-free solders [14]. Shen and Chan [15] also after studying Sn–9Zn composite solder with ZrO_2 nano-sized particles achieved significant improvements in mechanical properties. Recently, Al-Ganainy et al [16] investigated the effect of ZnO nano-particles on the structural and creep behavior of Sn-6.5 wt% Zn-3wt%In solder alloy. It has been found that a small alloying addition of ZnO nano particles has a beneficial effect on the microstructure. It improved the tensile creep properties of the ZnO-containing solder alloy.

It has been found that literature survey revealed that no studies have been reported so far on lead-free Sn-Zn solder joints containing Al_2O_3 nano-sized particles. So, the present work is devoted to investigating the effect of Al_2O_3nanometric particles is expected to be significant because the Al_2O_3 has no solubility in β-Sn matrix and could endure minimal growth and coarsening. Moreover, the Al_2O_3 nano-particles can offer an additional nucleation sites for the formation of refined IMCs. Therefore, this work investigates the effect of small addition of Al_2O_3 on the solidified microstructure, thermal properties and creep behavior of the Sn-5 wt% Zn solder alloy.

2. Experimental Procedure:

The investigated Sn-5 wt.% Zn solder alloy (hereafter termed alloy A) was prepared from pure materials 99.99%, by melting in air, the constituents in a Pyrex tube with a fluxing agent (colophony) to prevent the sample oxidation, in

electric furnace at 573 K followed by casting into a stainless steel mode. 0.5 wt. % with about 9 nm of Al_2O_3 (nano-particles) was mechanically incorporated (mexing) to part of prepared Sn-5 wt.% Zn lead free solder alloy to form new compound (hereafter termed alloy B). Both alloys were cold drown (withdrawn) to 0.75 mm diameter wire and working length of 50 mm for tensile creep testing and sheets of 0.4 mm thickness for structure investigations. The wire samples were annealed for 2 hours at 408 K, to eliminate the cold work acquired during swaging, then quenched in cold water at 273 K to have an identical thermal history. The microstructure studied by using scanning electron microscopy (SEM) JSM-5410, Japan. Differential scanning calorimetry (DSC) (shimadzu DSC-50) studied the melting process of the two samples. Heating rate for the specimens in DSC was 10^oC/min. For XRD, the crystal structure was studied by using a Philips diffractometer with wavelength CuK_α 1.54 ^0A during range $2\theta=10^0 - 80^0$. Testing tensile creep was carried out under different temperatures, ranging from 333 to 393 K, and different stresses, ranging from 10 to 25 MPa using a computerized tensile creep testing machine described elsewhere [17].

3. Results and Discussion:

3.1. Melting Characteristics:

The melting temperature (T_m) is critical issue needed in manufacturing to determine the usability of new solder alloys as in electronic devices. Fig. (1) shows the DSC curves of (plain solder alloy) and (composite solder alloy) upon heating at a scanning rate of 10^oC/ min. The DSC results are in Table 1.(T_m), (T_s) and (T_L) slightly decreased on doping with 0.5 wt.% Al_2O_3 particles, a little effect on the melting property was observed for plain solder alloy during the heating process. The reason may be that the reinforcing of nano Al_2O_3 particles modified the surface instability and the physical properties of grain boundary interfacial characteristics. Such particles may serve as restrained sites for solidification process as well as β-Sn. The pasty range property is very important for electronic applications. However, the pasty range, i.e., difference between solidus and liquidus temperatures, the pasty ranges are 10, 10.05 ^oC for plain and composite solder alloy, respectively. These values were found to be still lower than 11.5^oC for Sn–Pb solders [16]. It has been reported that a large pasty range may cause manufacturing problems, such as sensitivity to vibration during wave soldering [18]. Besides, the extensive pasty range may also increase the probability of fillet lifting phenomena, increases the tendency towards porosity and hot tearing due to the effect of alloy shrinkage and differential thermal contraction during solidification

3.2. Microstructure Analysis of Solder Alloy:

SEM images of Sn-5 wt.% Zn and Sn-5 wt.%Zn- Al_2O_3 solder alloys are shown in Fig. 2 (a,b). It is observed that the microstructure consists of the white

gray β-Sn matrix and the dark gray α-Zn phase in the form of fine particles, besides white gray spherical shaped consist of Al_2O_3 nano-particles as illustrated in Fig. (2b). For the plain solder alloy Sn-5 wt.%Zn showed refined and little existence of Zn phases while the particles of Zn phase was coalesced as large size existed in the samples alloy containing nano-particles. This can be due to the precipitated Zn in the Sn matrix. It is clear that the Al_2O_3 nano-particles may dispersed uniformly on the surface of the β–Sn grains in the solder matrix. From the EDX analysis for the specimen shown in Fig.2 (b,d) it can be concluded that the matrix contains β-Sn, α-Zn besides the Al_2O_3 nano-particles. The retardation effect of Al_2O_3 nano-sized particles, means that this addition of 0.5wt. % nano-sized particle suppressed and controlled the β-Sn grains dispersion of these nano-particles within the Sn-rich matrix producing the coarsening shape like microstructure with the β-Sn (Fig. 2b). This subsequently affects both physical and mechanical properties [19].

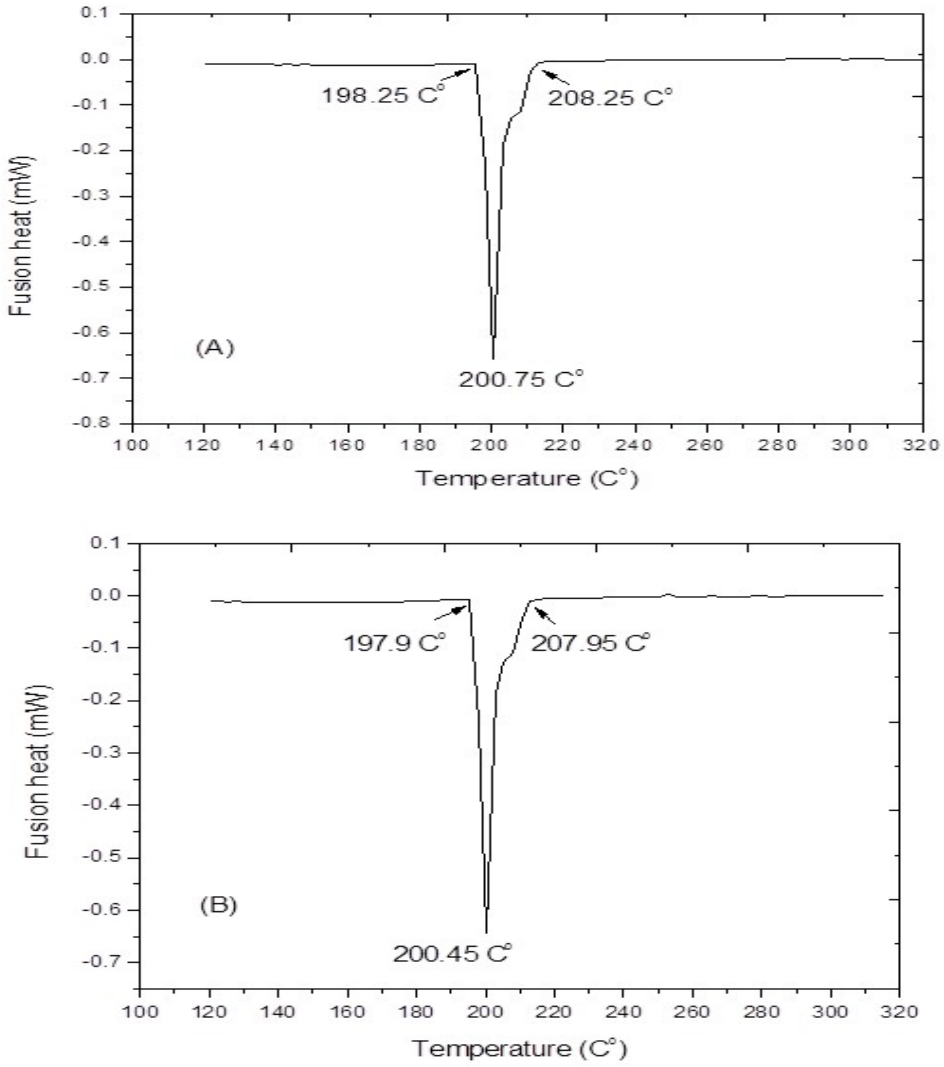

Fig. (1): DSC curves of (A (Sn-5 wt%.Zn) ,B (Sn-5 wt.%Zn-0.5 wt%.Al_2O_3 alloys

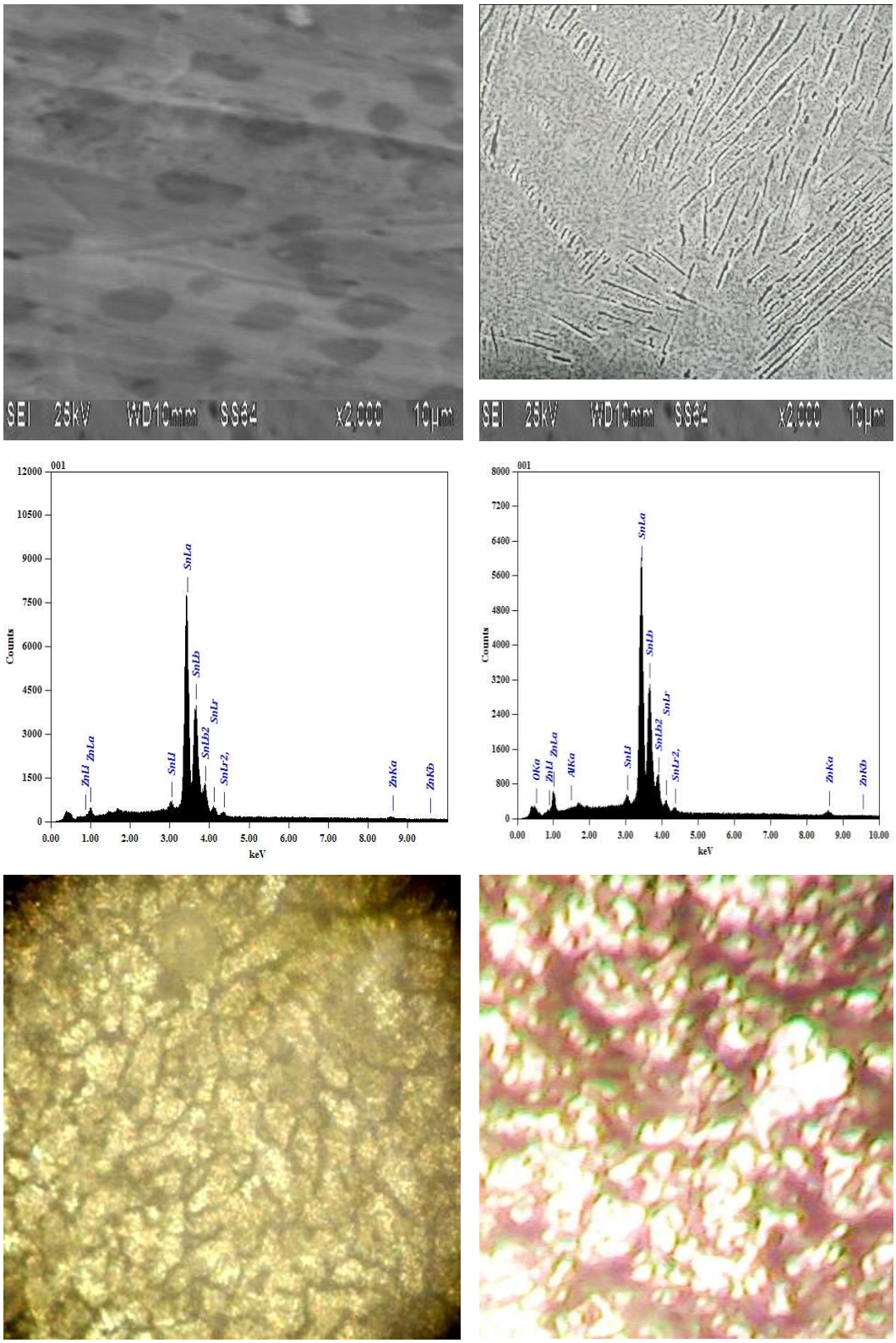

Fig. 2: SEM microstructure of (a) Sn-5 wt.% Zn ,(b) Sn-5 wt.% Zn-0.5 wt.% Al_2O_3, corresponding EDX analysis (c, d) and optical microscope (E,F) for plain and composite solder alloys, respectively

Table 1 : Comparison, of melting temperature (Tm), solidus temperature (Ts), liquidus temperature (TL) and pasty range of (alloy A) and (alloy B).

Alloy	T_m (^{o}c)	T_s (^{o}c)	T_L (^{o}c)	Pasty range (^{o}c)
Sn-5 wt.% Zn	200.75	198.25	208.25	10
Sn-5 wt.%Zn-Al_2O_3	200.45	197.90	207.95	10.05

X-ray diffraction patterns obtained for plain and composite solder alloy are given in Fig.3 (a,b). It can be observed that the plain solder alloy consists of two phases β-Sn matrix and α-Zn phase while the composite solder with Al_2O_3 nano-sized particles consists of β-Sn phase, precipitated α-Zn phase and the existence of nano-sized Al_2O_3 particles. This is in agreement with the results obtained by SEM and optical microscope given in Fig.2 (a,b,c,d,e,f).

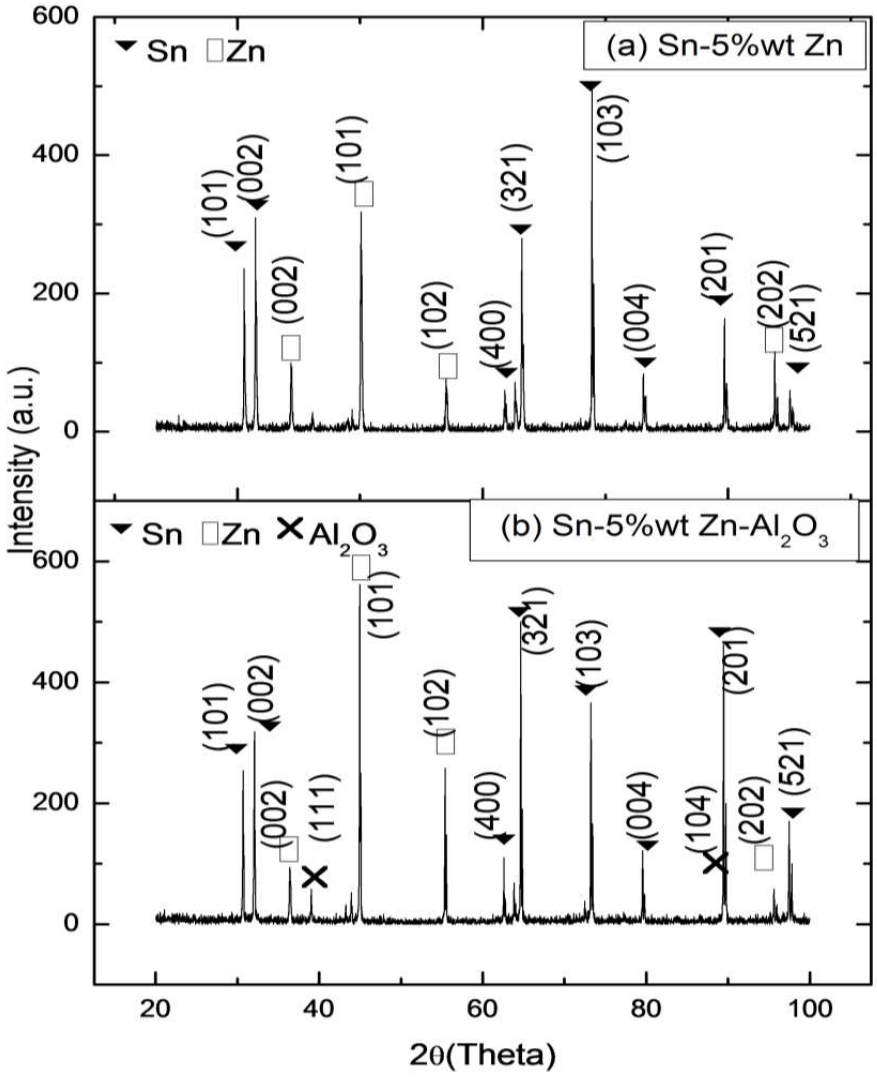

Fig. (3): XRD patterns of (a) Sn-5 wt. % Zn, (b) Sn-5 wt. % Zn-0.5 wt. % Al_2O_3

3.3. Creep Properties:

The phase diagram of this system [20] is relatively well established and a number of thermodynamic assessments are available for this simple eutectic system. At 198.5°C, the liquid decomposes into the two terminal solid solutions, (Zn) and (Sn). The tensile creep behavior of plain and composite solder alloys were carried out at the temperature range from 333 K to 393 K under the effect of applied stresses ranging from 10 to 25 MPa. Creep behavior of both samples was found to be strongly affected by the applied stress as has been observed in Fig.(4). These isothermal creep curves of both solders showed monotonic shift towards higher strains and lower fracture times on increasing the deformation temperature and / or the applied stress. Under the same testing conditions, the level of creep strain for composite solder alloy generally lower than that for the plain solder alloy.

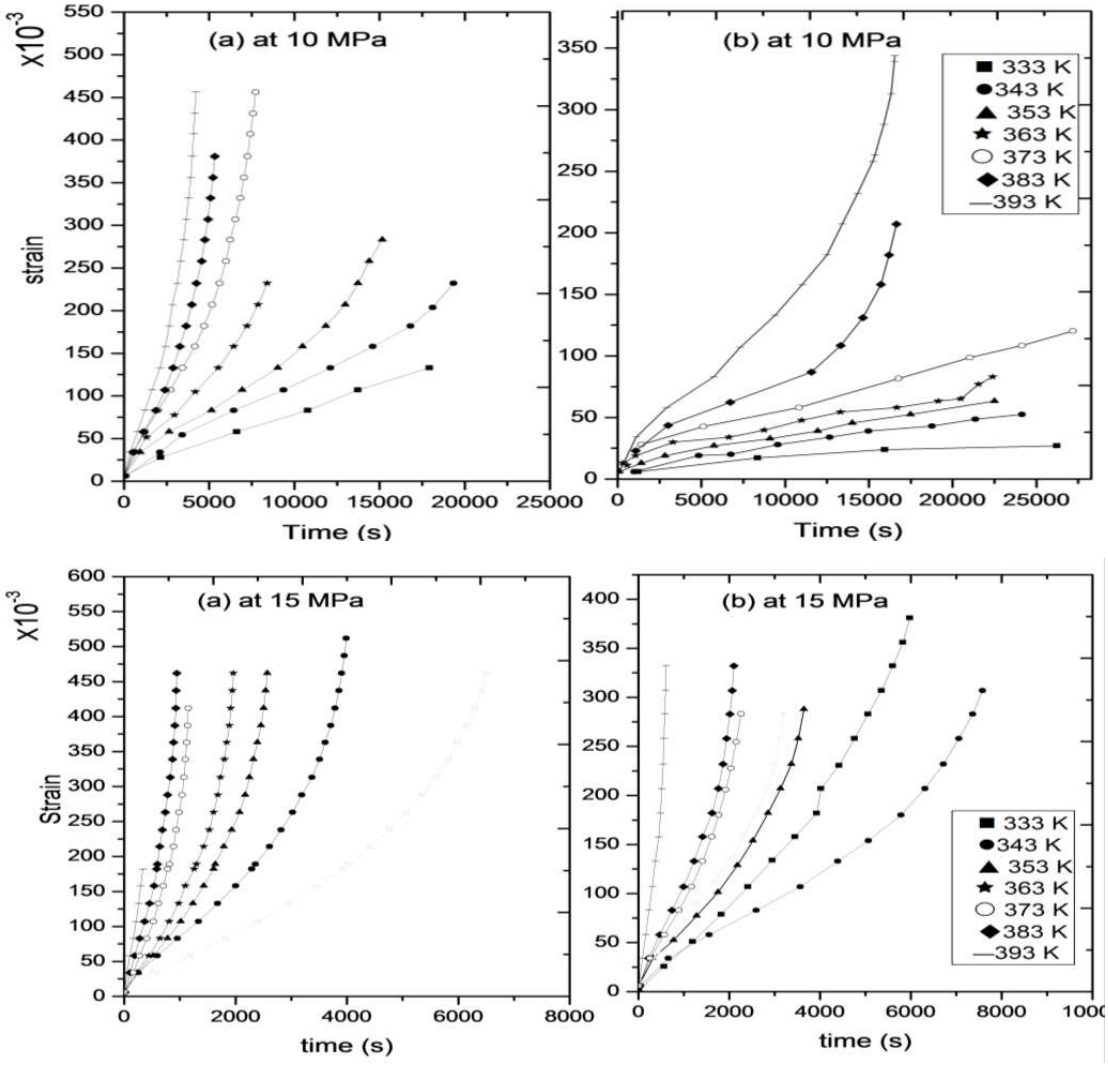

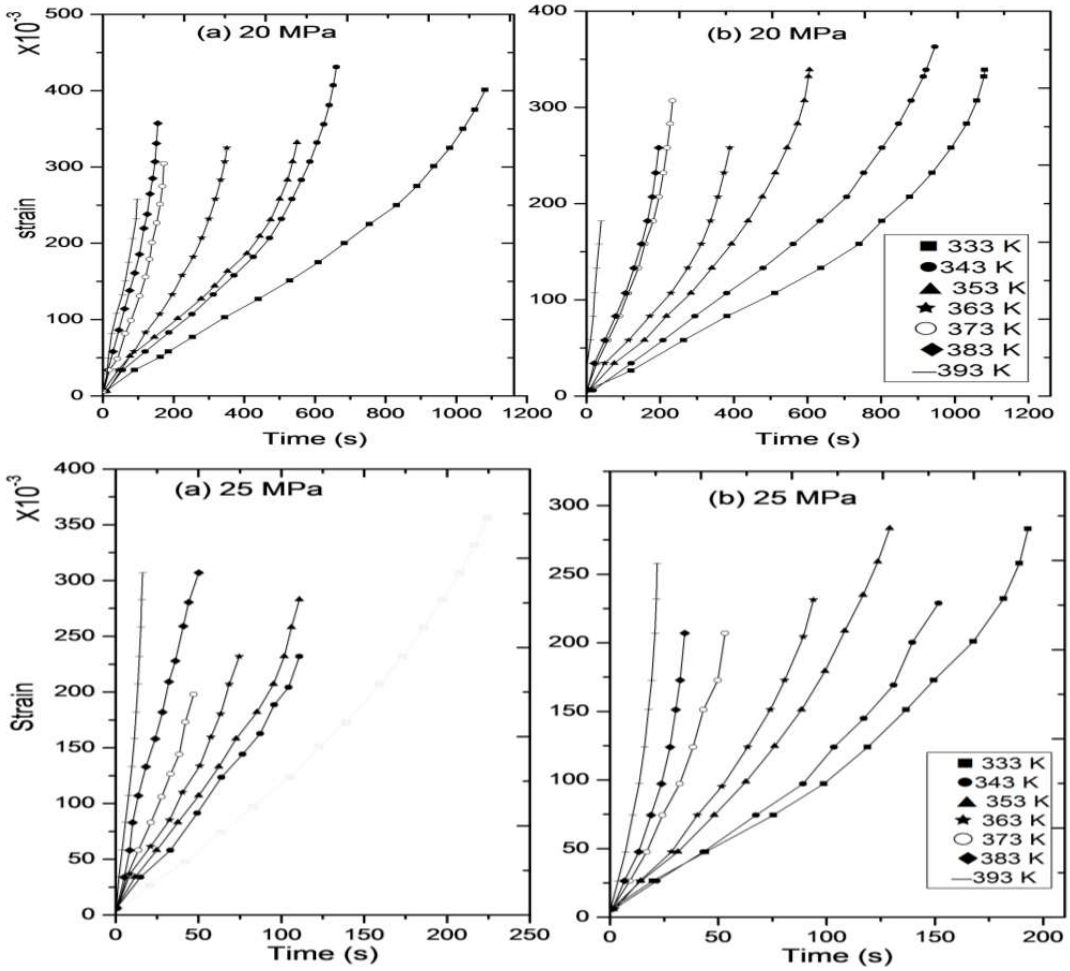

Fig. (4): Strain- time relations for both (a) plain and (b) composite solder at 10,15,20 and 25 MPa

The transient creep strain, ε_{tr} was found to obey a relation of the form [21],

$$\varepsilon_{tr} = \beta t^{n} \quad (1)$$

where ε_{tr} is the transient creep strain, and β,n are constants depending on the test conditions. From the relation between $\ln\varepsilon_{tr}$ and ln t given in Fig.5(a,b), at different temperatures under a certain stress of 10 MPa the parameter n is obtained as the slope of the straight lines and β is deduced from the intercept with ln εtr axis. The transient creep parameter n will increase with increasing testing temperature as has been observed in Fig.5(c). In addition, increasing the testing temperature T resulted in: (i) increasing thermal agitation for the moving dislocations leading to faster annihilation and/or (ii) decreasing the pinning effect of the pinning centers in each solder components. Hence the increase of n with T can be accounted. For higher values of n for the Sn-5wt% Zn composite solder compared with those in the Sn-5wt% Zn plain solder can be rendered to the decrease of the grain sizes in the composite solder compared with those in the Sn-5wt%Zn plain solder pointing to the integrated role of both grain size (Fig. 2 E,F) and deformation

temperature in decreasing the dislocation density ρ [22]. So the variation of β Fig. 5(d) and n Fig. 5(c) values are therefore thought to be due to the redistribution and rearrangement of dislocation in the network at transformation which lead to the formation of new Frank- Read Soures [23]. The activation energy of the transient creep, E, for both alloys was calculated using an Arrhenius equation of the form [24].

$$\beta=\beta.e\ (-E/KT) \qquad (2)$$

where β is a constant depending on the test conditions, K is the Boltzmann constant, T is the absolute temperature. The relation between ln β and 1000/T, is given in Fig. 6 (a,b), which gave straight lines for the different applied stresses. The experimental value of activation energy Q has been frequently used to identify the mechanisms controlling the deformation process. The value of Q for plain solder alloy (10.78 KJ/mole) is higher than composite solder alloy (8.74 KJ/mole) representative. Activation energies suggested that the dominant deformation mechanism in Sn–5 wt% Zn solders is diffusion motion.

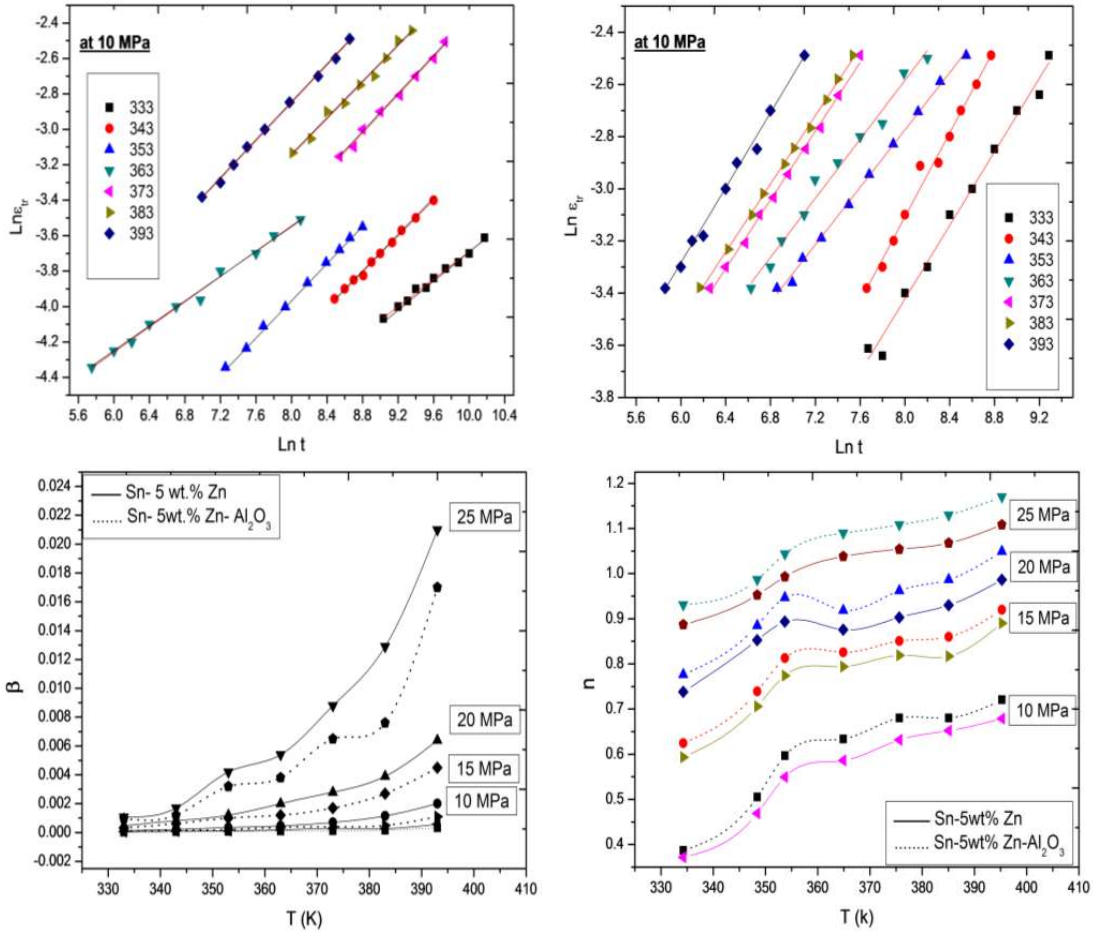

Fig. (5): Relation between ln εtr and ln t for different deformation temperatures for both alloys (a,b) and The temperature dependence of creep parameter (n) and (β) at (c,d) for both alloys, respectively.

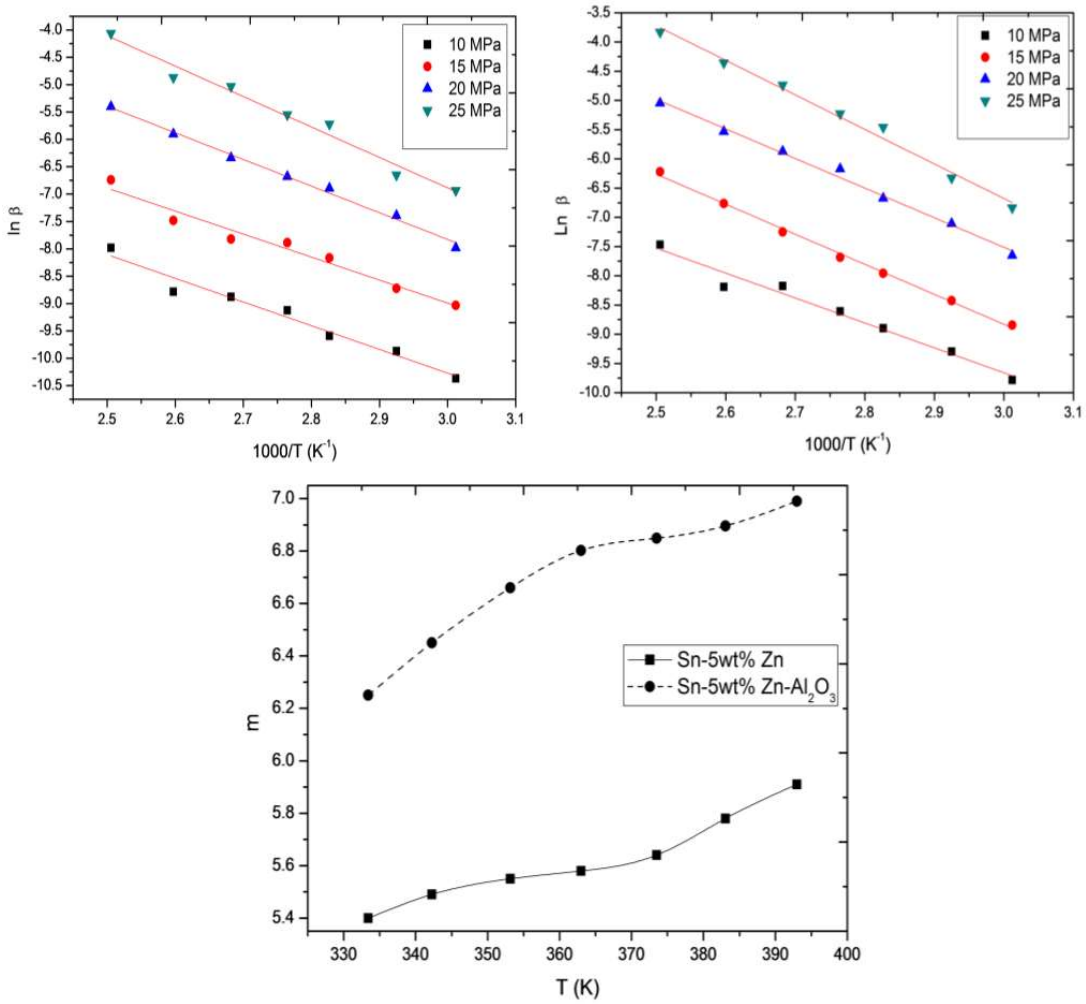

Fig.(6): The relation between Ln β and 1000/T for (a) plain and (b) composite solder alloy

The minimum (steady state) creep rate $\dot{\varepsilon}_{st}$ is one of the most important creep parameters for fundamental and engineering studies. Its stress dependence is often described by the power-law equation, $\dot{\varepsilon}_{st} = C\ \sigma^{m}$, where C is a constant and m is the stress sensitivity parameter (stress exponent), and both parameters were found to depend on the experimental test conditions. The steady state creep rate $\dot{\varepsilon}_{st}$ of the tested samples is calculated from the slopes of the linear parts of the creep curves that obtained at the different test conditions. It increased with increasing both the testing temperature and/or applied stress for both solders as observed in Figs. 7(a,b).

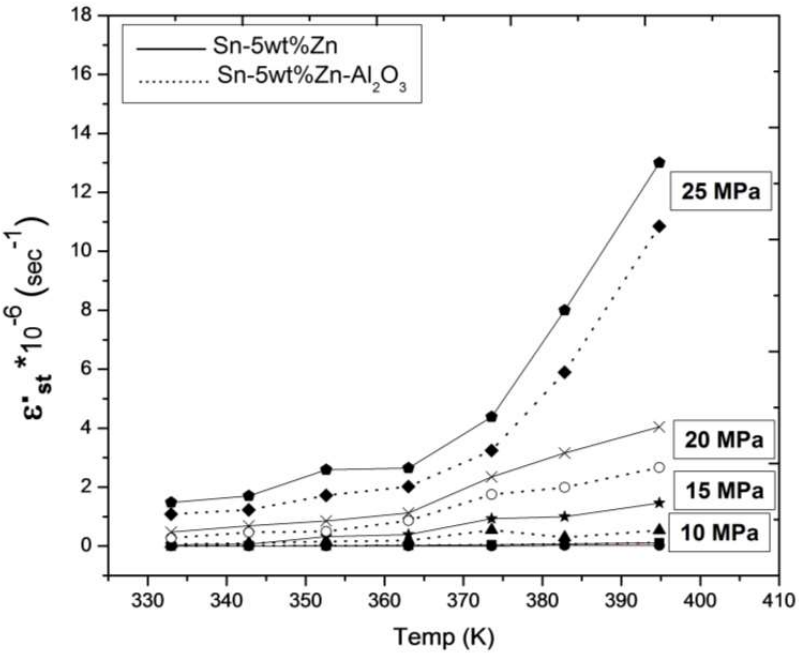

Fig. (7): Temperature dependence of the steady state creep rate $\dot{\varepsilon}_{st}$ and the stress sensitivity parameter (m) for both Sn-5wt%Zn plain samples and Sn-5wt%Zn composite sample alloys

In general, the mechanical response and performance of materials change with increasing temperature. A few properties and performance, for example, strength and creep resistance decrease with increasing temperature.

The transient and the steady creep stages are related to each other by the relation:

$$\beta = \beta_0 (\dot{\varepsilon}_{st}) \quad (3)$$

where β_0 is a constant and is the steady state creep exponent which measures the contribution of the transient mechanism to the steady state creep as in Fig. (8). Is measured as:

$$= \ln \beta / \ln \dot{\varepsilon}_{st} \quad (4)$$

The value of show to what extent the transient stage characteristics extend to the steady state creep. The density of dislocations at the end of the so-called sub-steady state creep in the middle of the primary creep state [22,25] increases within grains and near grain boundaries. These dislocations get into uniform distribution where the steady state creep stage starts.

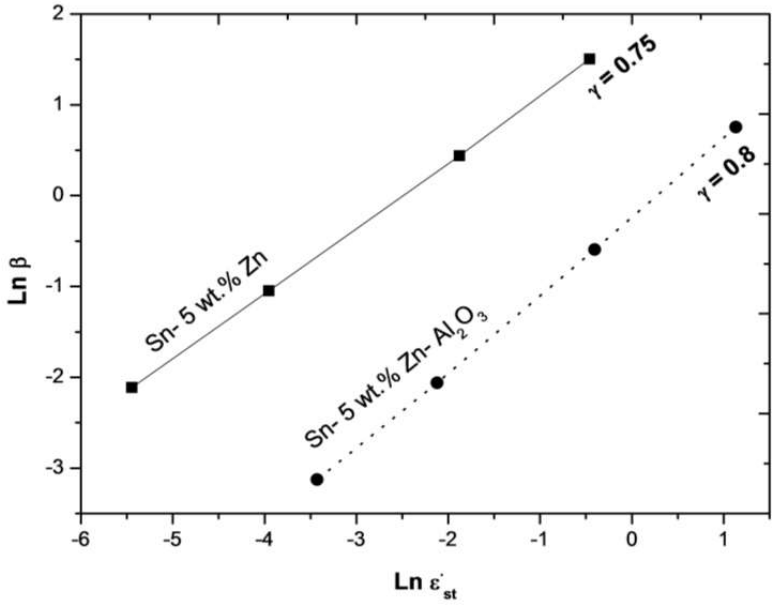

Fig.(8): The relation between Ln β and Ln $\dot{\varepsilon}_{st}$ for both Sn- wt.% Zn plain and composite solder alloy

We utilize an Arrhenius type equation of the form [26]

$$\dot{\varepsilon}_{st} = \text{const. exp } (-Q/KT) \qquad (5)$$

where k and T are Boltzmann's constant and absolute temperature, respectively. The creep-activation energy Q of the entire solders can be calculated in the mentioned temperature range (333-393 K), by linear regression of the experimental data relating ln $\dot{\varepsilon}_{st}$ and 1000/T (Fig.9). It shows that the calculated energy needed for the operating mechanism in the steady-state creep is 45.4 KJ/mol for the Sn-5wt%Zn plain and 25.4 KJ/mol for Sn-5wt%Zn composite solder ones. The energy activating the steady state creep was found to be dependent on the applied stress in both solders. These values suggest that the creep process at this stage is controlled by grain boundary sliding or migration mechanisms, which agree with previous finding [27]. The low value of the activation energy for the composite solder compared with that of the plain solder may be attributed to the difference in their microstructure. Therefore, it makes the alloy with nano particles is low cost. All the obtained creep parameters proved that adding Al_2O_3 is one of reasonable reasons for improving the creep properties of the composite solder.

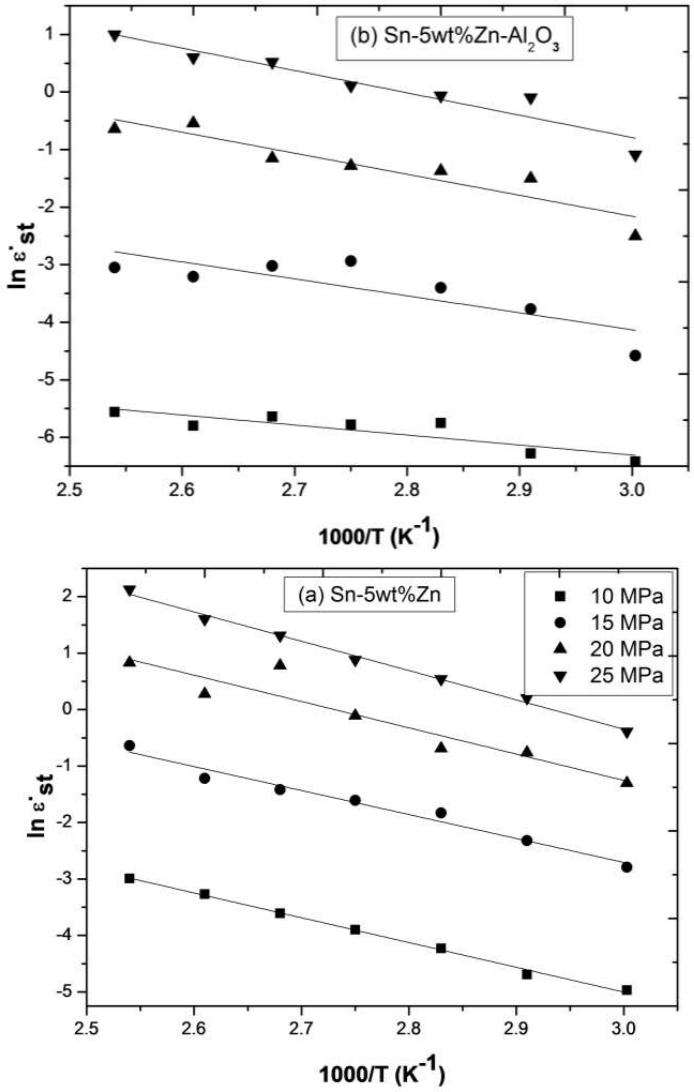

Fig. (9): Relation between (ε'_{st}) and 1000/T for Sn-5wt% Zn plain and composite solder alloy

Role of Nano-metric Al_2O_3 Particles in the Refinement Mechanism

It is generally known that microstructure stability is an important factor for improvement of solder reliability in electronic components. So, the effect of microstructure, which may vary during the life of the component, must be predictable. In short, the refinement mechanism of grains and suppression of the growth of IMCs in lead-free solders during solidification can be achieved by additions of nano-metric, non-reacting, non-coarsening oxide particles.

In order to precisely evaluate the influence of nano-metric Al_2O_3 particles on the microstructure and tensile creep properties of the solidified Sn-5wt%Zn solder we will refer to the optical micrographs shown in Fig. 2(E,F). It has been

found that addition of a small percentage of nano-metric Al_2O_3 resulted in refinement of the microstructure of the Sn-5wt%Zn composite solder Fig. 2(E,F). This refinement may be attributed to the adsorption of the nano-metric Al_2O_3 particles on the solidified grain surfaces through the matrix during the solidification process. The proposed mechanism for the effect of nano-metric Al_2O_3 particles on refinement of the β-Sn grains can be summarized as follows: during the solidification process, nano-metric Al_2O_3 particles, which are mechanically mixed with the Sn-5wt%Zn molten composite solder, cling to the micro-metric (larger-sized compared with those of the nano-mertic Al_2O_3 particles just as spheres cling to a plane. This can be simplified by treating the crystal surface as a plane and the nano-metric Al_2O_3 particles as spheres. Accordingly adsorption of such nano-metric surface active material can decrease the surface energy of the β-Sn, α-Zn [28]. Therefore, the growth rate of β-Sn grains was suppressed, resulting in a refined β-Sn and α-Zn phases. Second, this interpretation explains that the surface energy of the β-Sn grains decreased and suppressed the growth of the whole of β-Sn and α-Zn particles. From these standpoints, the obtained microstructure of the alloy B can reflect itself on the tensile creep properties and improvement the tensile creep resistance of the alloy B. This is because of the: (i) pinning action of these nano-metric Al_2O_3 particles which subsequently retards sliding of the grain boundaries and (ii) the dispersion strengthening mechanism of the matrix by the finely dispersed α-Zn and the nano-metric Al_2O_3 particles. These results were confirmed in a previous study [29,30] as well as in other studies [31, 32] (iii) Refinement of β-Sn grains that take place during the solidification process, will decrease β-Sn grain surface energy and retard the growth of the whole grain areas of the β-Sn matrix and help in controlling grain sizes and contribute very significantly to the material strength. In addition, grain boundaries greatly affect the creep resistance of materials. During the creep test, grain boundaries may cause strengthening or weakening depending on the deformation temperature and the applied stress. From the above analysis, it is not surprising that the addition of nano-metric Al_2O_3 particles to the plain solder makes composite solder joints more efficient in reducing the growth of the Zn particles in the temperature range used in this study.

4. Conclusion

In this work, the influence of adding nano-metric Al_2O_3 particles on the microstructure, thermal, and tensile creep behavior of Sn-5wt%Zn plain solder was investigated. The major findings are:

1. The nano-metric Al_2O_3 particles have been found to control the microstructure of Sn-5wt%Zn plain solder.
2. The tensile creep tests revealed an improvement in the creep resistance of the Sn-5wt%Zn composite solder.

3. The composite solder has longer creep life time while retaining higher creep resistance, indicating that the composite solder is suitable for solder fabrication.
4. The transient creep parameter n shows marked increase with temperature increase.
5. Steady state creep rate $\dot{\varepsilon}_{st}$ and the stress sensitivity parameter m were found to be increased with increasing both the deformation temperature and applied stress for both solders.
6. The high value of≈0.8, show that the initial state of the steady state creep is nearly totally the final state of the primary stage and that the controlling mechanism for the transient stage extends with a high degree to the steady creep stage.

I wish to express my deep gratitude to Prof. Dr. Radwan Hammoda Nada and Prof. Dr. Fakhry Abd El-Salam for their supervision and advice during the course of this work.

Reference:

1. Mc Cormak M, Kammlott GW, Chen Hs,Jin *S.Appl phys let* ; **65** (9): 1100 (1994).
2. Wade N, Wuk, Kuniij, Yamadas, Miyaharakk. *J. Electron Mater*, **30** (9): 1228 (2001).
3. Lang F, Tanaka H, Munegate O, Taguchi T, Narita T. Mater charact 24:223 (2005).
4. A.A.El-Dally, Y.Swilem, M.H.Makled, M.G.El-Shaaraway, A.M.Abdraboh, *J.Alloys compd.*, **484**, 134 (2009).
5. Barry BTK, Thwaites CT. Tin and its alloys and compound. New York: Wiley, 1983 (chap. 3,4).
6. X.Chen, M.Li, X.Ren, A. Hu, D. Mao, *J. Electron, Mater*., **35**, 1734 (2006).
7. Y. Kim, K. Kim, C. Hwang, K. Suganuma, *J. Alloys Compd*., **352**, 237 (2003)
8. G. Saad, A. Fawzy, E. Shawky, *J. Alloys Compd*., **479**, 844 (2009)
9. M. Sahin, E. ladırlı, J, Mater, Sci., **23**, 31 (2012)
10. M. Sahin, E. ladırlı, J, Mater, Sci., **23**, 484 (2012)
11. E. Cadırlı, U. B◌yük, H. Kaya, N. Maraşlı, J. Noncryst. *Solids*, **357**, 2876 (2011)
12. H. Mavori, S. Jin, *J. Electron. Mater*. **27**, 1216 (1998)
13. L.C. Tsao, S.Y. Chang, *Mater. Design* **31**, 990 (2010)
14. L.C. Tsao, S.Y. Chang, C.I. Lee, W.H. Sun, C.H. Huang, *Mater. Design* **31**, 4831 (2010)
15. J. Shen, Y.C. Chan, *J. Alloy. Compd*., **477**, 552 (2009)

16. Ventura T, Terzi S, Rappaz M, Dahle AK. *Acta Mater*, (4)**1651** (2011).
17. A.Fawzy, S.A.Fayek, M.Sobhy, E.Naser, M.M.Mousa, G.Saad, J. Mate821r. *Sci. Mater. Electron*., **24**, 3210 (2013).
18. L.C.Tsao, S.Y.Chang, Cl.Lee, W.H.Sun, C.H.Huang. *Mater. Des*., **31**, 4831 (2010).
19. El-Daly AA, Mohamed AZ, FawzyA, El-Taher AM. *Mater Sci*., Eng A **528**: 1055 (2011).
20. A.Fawzy, S.A.Fayek, M.Sobhy, E. Nasser, M.M.Mousa, G.Gaad, *Materials since & Engineering* A **603**, 1 (2014).
21. Hansen M, Anderko K. constitution of binary alloys. New York McGrew Hill Book Co. Inc,: P.337 (1958).
22. Friedel J. Dislocations. London: pergamon press; P.304 (1964).
23. G. Saad. A. Fawzy, E. Shawky. *J.Alloys compd*, **479**, 844 (2009).
24. G.S.Al-Ganainy, A.Fawzy, F.Abd El-Salam. *Physica* β **344**, 443 (2004).
25. Abd El-Khalek AM.physica β 2002; 315: 7.
26. A. fawzy, S.A. Fayek, M. Sobhy, E. Nassr, M.M. Mousa, G. Saad. *Materials Science & Engineering* A **603**, 1 (2014).
27. L.C. Tsao, S.Y. Chang, C.I.Lee, W.H.Sun and C.H.Huang, *Materials and Design,* **31**, 4831 (2010).
28. L.C. Tsao, S.Y. Chang, C.L. Lee, W.H. Sun, C.H. Huang, *Mater. Des*. **31**, **4831** (2010)
29. A. Fawzy, S.A. Fayek, M. Sobhy, E. Nassr, M.M. Mousa, G. Saad, *Mater. Sci. Eng*. A **603**, 1 (2014)
30. A. Fawzy, M. Sobhy, E. Nassr, M.M. Mousa, G. Saad, *J. Mater. Sci*. **24**, 3210 (2013)
31. Y. Shi, J. Liu, Z. Xia, Y. Lei, F. Guo, X. Li, *J. Mater. Sci*. **19**, 349 (2008)
32. M.J. Esfandyarpour, R. Mahmudi, *Mater. Sci. Eng*. A **530**, 402 (2011)